

# Accelerators and detectors

W. K. H. Panofsky and M. Breidenbach

Stanford Linear Accelerator Center, Stanford, California 94309

[S0034-6861(99)02002-4]

## I. SCOPE

The developing understanding of particle physics, especially in the past 60 or so years, has been largely paced by the evolution of high-energy accelerators and detectors. We restrict ourselves here to describing crucial developments in accelerators related to high-energy particle collisions. Similarly, discussion of detectors will be restricted to those associated with the accelerators and colliders covered.

There exist extensive reviews on our subject (Particle Data Group, 1996; see pp. 128 ff. for colliders and pp. 142 ff for detectors). While there are extensive reviews, detailed technical descriptions of accelerators and detectors in the peer reviewed literature are very incomplete; original source material is largely contained in laboratory reports and conference proceedings and most major accelerator installations have never been comprehensively documented.

## II. GROWTH PATTERNS OF ACCELERATORS AND COLLIDERS

Accelerators and colliders can be parametrized by a number of characteristics. The energy of a particle as accelerated in the laboratory is not what is relevant in determining the threshold for initiating a particular elementary-particle process. The center-of-mass energy  $E_{c.m.}$  of two colliding particles of rest masses  $m_1$ , and  $m_2$  and total energies  $E_1$  and  $E_2$ , respectively, is given by  $E_{c.m.}^2 = p_i p^i$  where  $p_i$  is the total four-momentum of the particles. For instance, if a proton of energy  $E_1 = \gamma m_1 c^2$  strikes a proton at rest, then  $E_{c.m.} = [2(\gamma + 1)]^{1/2} m_1 c^2$ . In the nonrelativistic limit only one-half of the incident kinetic energy is available, while in the relativistic limit  $\gamma \gg 1$  the center-of-mass energy grows with the square root of the energy of the incident protons. If two relativistic particles collide head on then  $E_{c.m.} = 2(E_1 E_2)^{1/2}$  or  $2E$  if the particles have identical energy. These relations demonstrate the energy advantage of colliding beams. But as investigations extend to smaller dimensions, the concept of what constitutes an elementary particle changes. At distances with the analyzing power of current colliders ( $10^{-18}m$ ) quarks and leptons are "elementary." Thus the relevant energy of a high-energy accelerator or collider defining its "reach" in initiating elementary-particle processes is neither the laboratory beam energy nor the collision energy in the center-of-mass frame of *composite* colliding particles, but is the collision energy in the frame of the center of mass of colliding "elementary" *constituent* particles.

The luminosity, defined as the data rate per unit cross section of the process under investigation, is another critical parameter. For high-momentum-transfer events the cross section is expected to vary inversely as the square of the momentum transferred. Therefore the luminosity of colliders should increase quadratically with energy in order to yield a constant data rate for "interesting" or novel events. In addition other parameters are of relevance to the experimenter, such as the background conditions, that is particle fluxes other than those originating from the collision under investigation. Then there is the "duty cycle" of the machine, which is the time structure over which collisions occur. Few modern accelerators or colliders produce random collisions uniformly distributed in time. Some accelerators are pulsed and most colliders employ bunches of particles rather than continuous beams. The resulting "duty cycle" limits the ability to interpret the time relationship among products of interaction. Experiments with accelerators use either the primary collisions or secondary beams produced in these collisions; the quality and quantity of secondary beams differ among types of accelerators and colliders.

Last, but unfortunately not least, is the matter of cost. The scaling laws that relate costs to growth of each technology define the historical growth patterns of accelerators and colliders. Figure 1 describes the growth over time of laboratory energy for various particle accelerators.<sup>1</sup> This pattern, first published by Livingston (1954), exhibits important features. An almost exponential growth of laboratory energy with time is fed by a succession of technologies; each technology saturates and is superseded by new technologies. In parallel with this pattern such new technologies have led to a decrease in cost per unit of laboratory energy by about four orders of magnitudes over the time period covered by Fig. 1.

The more relevant quantity describing the "reach" of accelerators into the unknown is the center-of-mass energy in the constituent frame, shown in Fig. 2. In this figure hadron colliders (proton-proton and proton-antiproton) and lepton colliders (electron-electron or positron) are plotted separately. The constituent center-of-mass energy of hadrons has been derated by a factor of about 6 relative to that of lepton colliders, to account for the hadron substructure of quarks and gluons. Needless to say, such a derating of colliders using "nonele-

<sup>1</sup>For a listing of the relevant machines, see the 1996 Review of Particle Physics (Particle Data Group, 1996). We shall cite here only machines at the frontiers of performance.

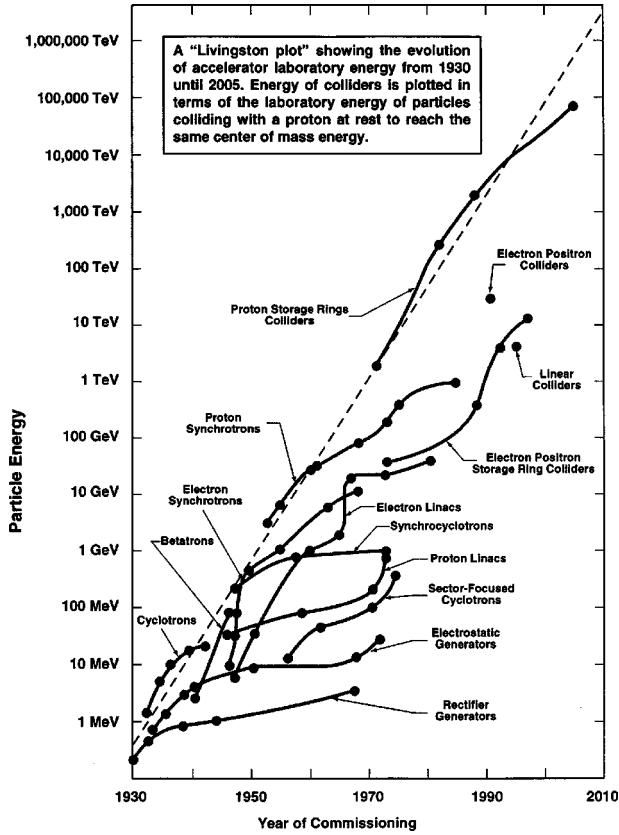


FIG. 1. A "Livingston plot" showing the evolution of accelerator laboratory energy from 1930 until 2005. Energy of colliders is plotted in terms of the laboratory energy of particles colliding with a proton at rest to reach the same center-of-mass energy.

mentary" particles can only be an approximation. The internal dynamics of the substructure of composite particles can permit a lowering of reaction thresholds, albeit accompanied by a decrease in luminosity. Again, an exponential growth has apparently been sustained over the limited period of time over which colliding-beam devices have been successfully constructed, and that growth is comparable for hadron and lepton colliders.

Particle beams striking stationary targets of condensed matter produce effective luminosities many orders of magnitude larger than those attainable by colliding beams. The luminosity growth of colliders is shown in Fig. 3. Thus far this growth has not matched the quadratic growth with energy required to maintain constant data rates.

III. PRINCIPLES, CATEGORIZATION, AND EVOLUTION OF ACCELERATORS AND COLLIDERS

Fundamentally accelerators are either electrostatic machines, in which particles are accelerated by traversing a difference in electrical potential once, or they are transformers, which repeatedly use high-current low-voltage circuit elements to supply energy to a high-voltage low-current accelerating path.

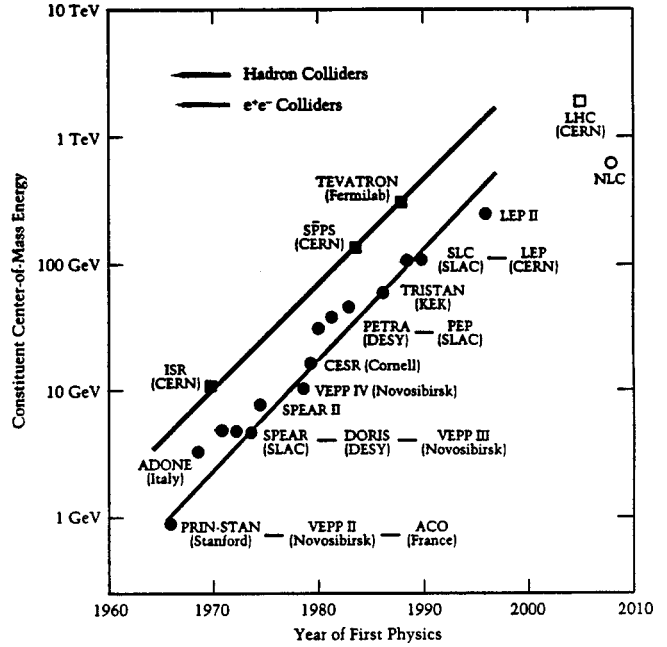


FIG. 2. The energy in the constituent frame of electron-positron and hadron colliders: filled circles and squares, constructed; open circle and square, planned. The energy of hadron colliders has here been derated by factors of 6–10 in accordance with the fact that the incident-proton energy is shared among its quark and gluon constituents.

A. Electrostatic devices

Early accelerators were discharge tubes fed by conventional high-voltage sources. Limitations arose in the ability of the discharge tubes to sustain high voltages and in the availability of high-voltage sources. The Tesla-coil accelerators were resonant step-up transformers with both primary and secondary resonating at the same frequency. Cascade accelerators, pioneered by

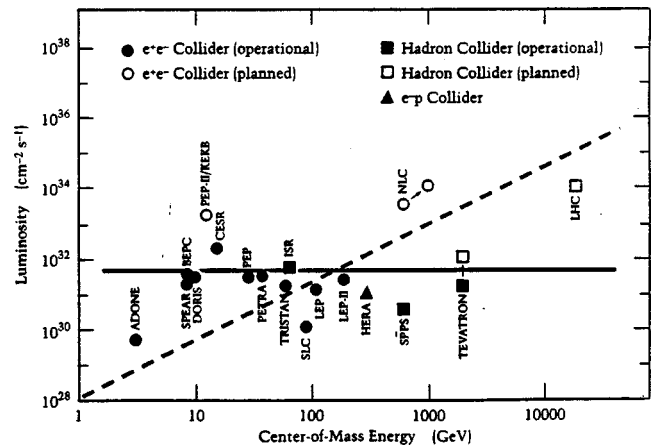


FIG. 3. Peak luminosities achieved at existing colliders and values projected for planned or upgraded machines: dashed line, luminosity increasing as the square of the center-of-mass energy. Note that the rated machine energy has been used in calculating the abscissa. Data updated courtesy of Greg Loew, SLAC.

Cockroft and Walton (1932), were able to attain voltages in the several hundreds of kilovolts by charging capacitors in parallel and reconnecting them in series. In the Van-de Graaff generator (Van de Graaff, 1931) charges were sprayed onto a moving belt and then removed inside a high-voltage electrode; this device reached energies near ten million electron volts. The design of discharge columns evolved to permit better voltage distribution and focusing, and vacuum practices improved. Electrostatic generators continue to be produced for research in nuclear physics and for medical uses.

## B. Transformers

Energies above about 10 MeV are not attainable electrostatically. The most important early development to exceed that limit was the cyclotron proposed by Lawrence and Edlfsen (1930) and put into practice by Lawrence and Livingston (1932) using the well-known principle that the orbital period of nonrelativistic charged particles circulating in a uniform magnetic field is independent of energy. Thus if a radio-frequency voltage matching the revolution frequency is applied across a gap placed in such a field, then the particle will gain energy and will spiral out in the magnet.

Cyclotrons developed rapidly in the period before World War II but the decrease in orbital frequency as the particles become relativistic limits the attainable energy. Focusing was first addressed by empirical “shimming” of the magnetic field. A more analytical approach initially by Steinbeck (1935) showed that focusing both horizontally and vertically could be obtained by a small radial decrease of the magnetic field, thus generating a further decrease in orbital frequency. These decreases in orbital frequency can only be overcome by extremely high radio-frequency voltages so that the desired energy can be attained in relatively few orbital turns. The 184-inch cyclotron in Berkeley was designed accordingly to attain deuteron energies above 100 MeV but the machine was diverted to military purposes as an isotope separator. In the meantime discovery of the phase stability principle discussed below made this brute force approach unnecessary.

The cyclotron principle fails for electrons, whose motion becomes relativistic at moderate energies. The betatron, invented by Wideroe<sup>2</sup> and first put into use by Kerst (1940) was a transformer in which the energy of electrons in circular orbits was increased by the induced electric field from an increasing flux in a central iron core driven by appropriate windings. The required average magnetic field in the drive core had to be twice that of the radially decreasing magnetic field at the orbit of the betatron. Betatrons reached an energy up to about 300 MeV, limited by the radiation loss per turn, which cannot be compensated in a betatron.

<sup>2</sup>For a full discussion of the complex of inventions and demonstrations leading to the betatron see; Waloschek (1994).

In a *linear induction accelerator* individual iron cores are stacked axially and excited through separate driving circuits. This principle permits acceleration of very-high-intensity electrons, in the kiloamp region (Christofilos *et al.*, 1964). Such devices are still used as x-ray-sources for diagnosis of rapid dynamic systems. A linear radio-frequency accelerator was developed by Sloan and Lawrence (1931), in which an alternating rf voltage was applied across a succession of gaps traversed by a beam, limited to low-velocity heavy ions by the low frequency of available rf sources.

A dramatic extension of accelerators and colliders to high energies was made possible by conceptual and technical developments.

### 1. Phase stability

Phase Stability was invented independently by McMillan (1945) and Veksler (1944).<sup>3</sup> In the pre-World War II accelerators synchronization between the rf fields and the particle bunches was achieved by “dead reckoning” McMillan and Veksler recognized that the phase of the accelerating rf voltage could be stably “locked” into synchronization with the transit time of particle bunches under appropriate conditions. In a circular accelerator such stability is achieved by the particle bunch’s crossing an accelerating gap during either a descending or ascending part of the radio-frequency voltage, depending on the relation between orbital path length and orbital momentum. This relation depends on the focusing mechanism and the relativistic mass. In a linear accelerator such stability is achieved by accelerating the bunch during the *ascending* part of the radio-frequency voltage. Such stability permits “synchrotron oscillation” about a stable phase.

The principle of phase stability led to diverse applications. In a synchrocyclotron particles are injected into a static magnetic field and are accelerated by a radio-frequency source whose frequency decreases to match the revolution frequency as the energy, and therefore the relativistic mass, increases and as the magnetic field weakens as the particle spirals out. Under this condition the particles remain phase locked to the electric field.

In a synchrotron particles are injected into a rising magnetic field and traverse a radio-frequency cavity excited at a near-constant frequency.<sup>4</sup> A magnet of only small radial aperture is needed. The particles remain locked in stable phase while their energy, but not their radius, increases with the magnetic field. This is the principle of all of today’s high-energy circular electron and proton accelerators, including LEP (at CERN), the world’s highest-energy electron collider (nearly 100 GeV per beam) and the Tevatron at Fermilab, the world’s highest-energy proton collider. The latter is to

<sup>3</sup>Described within the USSR in 1944; published in English in 1945.

<sup>4</sup>If injection into a synchrotron is at a particle velocity not fully relativistic, the frequency can be slightly modulated, for instance by loading of the accelerating cavity with ferrite.

be followed by the Large Hadron Collider at CERN, designed to attain a proton energy per beam of 7 TeV.

All modern *proton linear accelerators* use phase stability and continue to be the devices of choice as injectors into today's proton synchrotrons. They operate as accelerators in their own right up to about 1 GeV where high intensity is required.

## 2. Strong focusing

Strong focusing was adapted to synchrotrons independently by Christofilos (1950), and by Courant, Livingston, and Snyder (1952). Focusing in earlier circular machines was attained through radial falloff in the magnetic field; electrostatic focusing or magnetic solenoids provided focusing in linear accelerators. "Strong focusing" originated from the realization that if a diverging and a converging lens of equal and opposite focal strength are separated by a finite distance, then the net focusing effect is positive. A magnetic quadrupole produces focusing in one plane and defocusing in the plane at right angles. Thus two quadrupoles separated by a finite distance and rotated by 90 degrees relative to one another focus in both planes. This focusing strength varies quadratically with the magnetic-field gradient in the quadrupoles and can be much stronger than that of solenoids or that of radial magnetic-field gradients.

Strong focusing drastically decreases the needed aperture of proton and electron synchrotrons and of linear accelerators. Thus strong focusing greatly extends the range of particle energies that can be economically attained.

Strong focusing results in particle oscillations about a central orbit whose wavelengths are generally shorter than the circumference of the circular accelerator. This creates the possibility of resonances between such focusing oscillations and harmonics of the basic orbital frequency. Moreover, the region in accelerating phase for which phase stability exists can change sign, leading to a transition energy at which phase stability vanishes. Such problems can be avoided by appropriate design of the "lattice" of the focusing elements and by rapid passage through transition.

Proton and electron synchrotrons have been configured into colliders, leading to obvious center-of-mass advantages. Circular colliders are composed of storage rings, which are synchrotrons storing beams after the magnetic field has reached its final value. Stored electrons require compensation of the radiation loss by cavity reacceleration. Synchrotron radiation loss of protons is still negligible even at the highest energies attained today, but will become of future importance.

All modern circular colliders use both phase stability and strong focusing. Circular electron-positron colliders incur a radiation loss per turn which scales as the fourth power of the energy divided by the orbit radius. If the costs growing linearly with radius are matched with those scaling with the energy loss per turn, then the total cost of an electron-positron collider will grow with the square of the energy. The 27-km circumference electron-positron collider at CERN will probably be the

highest-energy electron circular collider ever built. Collisions between linear accelerator beams and beams stored in a storage ring have been considered but thus far studies do not project competitive luminosity.

## 3. High-impedance microwave devices

W. W. Hansen (Ginzton, Hansen, and Kennedy, 1948) invented the electromagnetic cavity in 1937 with the goal of generating high voltage at moderate input power. The invention led to amplifiers, oscillators, cavities to compensate energy loss in circular accelerators, and linear accelerators, among them the disk-loaded waveguide. When such a waveguide is operating as an electron accelerator, the phase velocity of a propagating wave in this structure is matched to the particle velocity. The group velocity is tailored to provide a filling time compatible with the pulse length of the radio-frequency source, so as to provide an appropriate profile of accelerating voltage versus length. The highest-energy electron linear accelerator is the SLAC machine operating up to 50 GeV. Beyond that, linear colliders in which an electron beam from one linear accelerator collides with a beam accelerated by a separate machine are the most promising developments to exceed electron-positron energies attainable by circular storage rings. They require high average beam powers and exceedingly small beam cross sections in order to attain the required luminosity. The SLAC linear collider produces collisions between 50 GeV electrons and positrons.

## 4. Superconducting technology

The availability of superconducting materials made another gain in particle energy possible. For electromagnets the material of choice has been niobium-titanium, which can be fabricated into multistrand cables designed to minimize losses during magnetic field changes. Niobium-tin can sustain higher magnetic fields, but its mechanical brittleness has thus far prevented extensive use. The new high-temperature superconductors have only limited application in high-energy physics, restricted to connections and leads. After extensive development, solid niobium or niobium coatings inside radio-frequency cavities have become practical and reliable and serve as accelerating cavities, both in linear accelerators and as accelerating elements in proton and electron synchrotrons.

## IV. ACCELERATOR AND COLLIDER LIMITATIONS

Continued growth of accelerators and colliders is limited by technical and economic factors. Technical limitations are in the following categories:

(1) Material limits. Vacuum breakdown and field emission are controlled by practical factors such as surface irregularities, dielectric inclusions, whisker growth, and so forth. These limit gradients in linear accelerators and in accelerating devices in synchrotrons.

Magnetic fields in “warm” magnets are limited by the saturation of iron, while those in superconducting magnets are limited by quenching of the superconducting materials in magnetic fields and by the problems inherent in restraining the large forces on conductors in such magnets. Frontiers in this respect have been advanced by the use of supercooled helium and by metallurgical advances in the production of superconductors and cables.

(2) Nonlinear dynamics and collective effects. The previous sketchy discussion has focused on the behavior of “free-space” single particles in “ideal” externally generated electric and magnetic fields. Such motions will be modified by the electromagnetic fields generated by induced currents in metallic envelopes, by deviations of fields from the ideal, generally linear, form, and by collective effects of particle groups on the motion of a single particle.

Induced fields and the collective fields of a bunch generate a “wake field” that affects individual particle orbits, both longitudinal along the motion of the particles and transverse to that motion. Wake fields not only affect the shape of a bunch of particles, in that the fields produced by the head of a bunch affect the motion of its tail, but they also can result in electromagnetic coupling between successive bunches in an accelerator. In the transverse direction such effects can produce decreased luminosity and outright instability. Luminosity decreases when wake fields dilute the phase-space density of the particles in a bunch. Instability can result if transverse displacement of preceding particles induces wake fields which successively deflect succeeding particles further. Such phenomena are complex.

Longitudinal wake fields result in the lengthening of the particle bunch in an accelerator. This can counteract efforts to maximize luminosity in a collider using very-short-focal-length magnets near the interaction region, since shortening of the focal length will be ineffective if the bunch length is too large. Transverse instabilities are particularly serious if the transverse displacement of the particle induces fields in either engineered or inadvertent resonant structures. The transverse displacement can induce so-called “higher-order modes” in such structures; any discontinuity in a vacuum envelope can enhance transverse wake fields.

The effect of transverse wake fields can be counteracted by a number of measures. The discontinuities in vacuum envelopes can be minimized; focusing strength can be enhanced, thus limiting transverse excursions; the frequency of transverse focusing oscillations can be dispersed among successive sections in a radio-frequency linear accelerator, thus damping a resonant buildup of transverse motion.

The coupling among particle bunches can become coherent as the wavelengths of the Fourier component of the electromagnetic field become comparable to the dimensions of the particle bunch. In this event fields will act coherently and the forces correspondingly increase. The principal countermeasure against coherent instabilities is external feedback: The electromagnetic field of

the particle bunch is sensed by appropriate electrodes and is fed back to deflecting electrodes with a phase to damp the motion. Additionally structures can be designed which damp the relevant higher-order modes.

(3) Beam-beam interaction. Collisions between intense bunches of particles produce electromagnetic forces of one bunch of particles in the other. These forces shift the frequency of the focusing oscillations. If this “tune shift” becomes too large, then the frequency of radial focusing oscillations can shift into regions of instability, as discussed above. Actually the limiting tune shift is set, generally empirically, by nonlinear effects in the beam-beam interaction. Thus the permissible tune shift is subject to practical limits, which can be minimized by optimized design of the focusing lattice and shaping the beam profile during collision. In addition to the tune shift, the beam-beam interaction in electron-positron linear colliders also produces electromagnetic radiation as each particle experiences the collective electromagnetic field of the opposing bunch. Radiative effects broaden the energy spectrum of the colliding beams, thus making them less useful in elementary-particle physics experiments, and they also produce electromagnetic background.

(4) Beam-“vacuum” interactions. Interaction of the beams with residual gases or charge clouds in the vacuum can produce background. In addition, if electromagnetic radiation from synchrotron radiation or beam-beam interactions impact the vacuum wall, photoejected electron clouds affecting particle motions can be formed. Recent analyses (Raubenheimer and Zimmerman, 1995) show that this can lead to serious instabilities, in particular for the highest-energy proton-proton colliders.

(5) Injection. The design of ion sources in the case of hadron colliders and design of either thermionic or photocathodes in the case of electron machines can affect luminosity. In particular, space-charge effects at injection are limiting.

According to Liouville’s theorem, the invariant emittance, that is, the phase-space density times the relativistic factor  $\gamma$ , cannot decrease during acceleration, storage, or final interaction in a nondissipative system. Liouville’s theorem can be violated if damping takes place in the motion subsequent to injection. Such damping can be produced by emission of synchrotron radiation. This fact is utilized in damping rings inserted at an appropriate step in an accelerating cycle. Damping can also be accomplished by beam-to-beam cooling, in which an external beam of small phase volume is permitted to interact with the beam of the accelerator and exchange momentum. Finally damping can be accomplished by feedback in a circular machine by picking up signals from radial excursions and feeding those back onto the orbit at subsequent turns.

Thus the final luminosity may or may not be limited by the phase space at injection, depending on the presence of damping mechanisms.

## V. FUTURE COLLIDER POSSIBILITIES

The previous discussion outlined the principles underlying past and present accelerator and collider systems and identified installations at the current frontier. Existing technology permits limited extension but major advance depends on new technology.

Along conventional lines further extension in energy attainable by large circular hadron-hadron colliders beyond the Large Hadron Collider and larger linear colliders fed by traditional electron and positron linear accelerators appears feasible. Such machines can also become the basis of electron-electron and photon-photon colliders at high energies.

Hadron colliders beyond the Large Hadron Collider face economic limitations and must take synchrotron radiation into account. Therefore such machines require large radio-frequency power and have to face the potential of charge cloud and other instabilities discussed above. At the same time synchrotron radiation will provide damping, which may be beneficial in reducing instabilities.

An international effort is addressing construction of a large linear collider, possibly approaching the TeV per beam range. Leading candidates to feed such a device are conventional microwave linear accelerators operating at higher frequency than now in use. In addition superconducting linear accelerators are being explored, aiming at improvements in economy and gradient beyond current experience. Finally, there exists the possibility of feeding a linear collider by variants of a two-beam-accelerator principle. Here a high-current, low-voltage linear accelerator fed by induction or low radio-frequency sources drives a high-energy, high-gradient machine. Energy from the driver is coupled through appropriate transfer structures into the high-energy accelerator.

Substituting muons for electrons in circular machines reduces radiation by a large factor, while strong and weak interactions of muons appear identical to those of electrons. While the idea is old (Tinlot, 1962; Budker *et al.*, 1969) optimism has grown that muon colliders of adequate luminosity and background conditions can be designed. Luminosity depends both on initial muon yields and on cooling of the muons resulting from pion decay in a practical manner. The background problem is serious due to the large electron fluxes originating from decay of muons in orbit, and even decay neutrinos pose a substantial hazard.

In addition to devices based on extrapolations of established practice, new technologies are being analyzed. All of these, to be useful for high-energy physics, would have to be configured into linear colliders and therefore would have to generate both high energy and high average beam powers. Current research focuses on acceleration by very large intrinsic voltage gradients. Among these are devices using the high fields in intense laser beams (Channell, 1982). The electromagnetic field in a laser wave in free space cannot accelerate charged particles and therefore research addresses special geom-

tries which generate longitudinal electric-field components. Possibilities are the electric field when optical laser beams are diffracted from gratings, when coherent laser beams are crossed to generate a longitudinal-field component and similar geometrical arrangements. Other methods utilize the high electric fields contained in plasmas (Schoessow, 1994), the high gradients in the wake fields produced by intense particle bunches, and finally the extremely high electric fields that could be generated if plasma waves were excited in crystals (Chen and Noble, 1986); these could be used to accelerate particles channeled in such crystals.

## VI. PHYSICAL PROCESSES IN PARTICLE DETECTION

Charged and neutral particles interact with detector material via limited processes. Charged particles ionize any medium and can radiate Cerenkov, synchrotron, or transition photons. The ionization density, and consequently the rate of energy loss ( $dE/dx$ ) of charged particles in matter, is in essence a measure of particle velocity (Bethe, 1932; Bloch, 1933). Therefore measurements of ionization density in combination with deflection in a magnetic field (which determines the ratio of particle momentum to charge) can result in determination of rest mass. The ionization as a function of particle velocity  $\beta c$  has three regions: (a) a low-velocity region where the ionization decreases roughly as  $\beta^{-2}$  and then levels off to a region of (b) minimum ionization and (c) a region of logarithmic growth (relativistic rise) which reaches a plateau with  $\beta\gamma$  defined by the dielectric properties of the material, affecting the relativistically contracted electromagnetic field in its ability to ionize remote atoms.

Neutral hadrons may interact strongly to produce charged particles. Photons may interact electromagnetically via Compton scattering, photoelectric effect, or pair production. Neutrinos can generate charged particles with very small cross sections via the weak interaction. At high energies strongly interacting particles produce cascades, and electrons and photons produce electromagnetic showers. Ultimately any detector either senses ionization caused by primary or secondary charged particles or detects secondary photons by photoelectric mechanisms.

## VII. DETECTOR COMPONENTS

### A. Pictorial detectors

Pictorial Detectors utilize the particle track left by ionization and process the image of that track into a photographic or digital record.

The earliest track detector was the *cloud chamber*, which can either produce super saturation following an expansion of water vapor or it can be a continuously sensitive diffusion chamber in which a thermal gradient in water vapor leaves a region where condensation forms around an ionizing track. Subsequently photographic *emulsions* were specifically tailored through en-

hanced silver content to reveal, after development, particle tracks which are microscopically scanned. A *streamer chamber* produces conditions in which ionization in a gas generates enough light through ion recombination to permit photographic recording. In a *spark chamber* local breakdown occurs between high-voltage electrodes; the sparks can be photographed in a sequence of gaps between electrodes leading to a track in a photograph. In a *bubble chamber* a liquid is expanded leading to a superheated condition; gaseous bubbles will be formed along an ionizing track, which can be photographed.

All these devices greatly contributed to elementary-particle physics. Cloud chambers have been major tools in cosmic-ray research, including the discovery of the positron. Bubble chambers recorded associated strange-particle production and established the foundation of hadron spectroscopy. A limitation of bubble chambers and cloud chambers is that they cannot be “triggered”; they record *all* ionizing events irrespective of whether the events are novel or are signatures of well-known processes. However, photography can be triggered to select only events of current interest to limit labor in data analysis. Spark chambers and streamer chambers can be triggered but have inferior location accuracy. All pictorial devices other than the spark chamber permit measurements of ionization density.

Pictorial devices require substantial effort in data analysis; images have to be scanned either manually, semiautomatically, or totally automatically; tracks have to be reconstructed and hypotheses as to the event that may have occurred have to be fitted to the track pattern.

Pictorial devices have largely disappeared from use in elementary-particle physics. They cannot handle events produced with small cross sections in the presence of large uninteresting background. They tend to be expensive considering the data-analysis effort. Resolving time is generally long. Yet the slowest of these detectors—photographic emulsions—are still in use for elementary-particle physics because of their unexceeded track resolution of near one micrometer. Large emulsion stacks continue to be used in connection with neutrino experiments. Auxiliary electronic detectors can limit the emulsion area to be searched for precise vertex measurements.

## B. Electronic detectors

### 1. Scintillation counting

Suitably doped plastics have long been utilized for position measurement, time-of-flight measurement,  $dE/dx$ , and calorimetry. The scintillation photons from inorganic crystals and wavelength-shifted photons from plastic scintillators can either be detected by photomultipliers as high-gain, low-noise amplifiers of the electrons emitted by the photocathode or by suitable solid-state photodetectors. Issues of the number of separate measurements required, operation in magnetic fields, quantum efficiency, size, and cost determine the choice

of photodetector. Scintillators and photomultipliers still excel at precision timing in applications with modest spatial resolution requirements. For example, in the proposed Minos neutrino detector (Wojcicki, 1998), solid scintillator bars couple their scintillation light to optical fibers using wavelength-shifting dopants in the fibers. A variant is the Fiber Tracker, in which optical scintillator fibers form large arrays, with each fiber having an independent photodetector (DO Upgrade, 1996).

### 2. Wire drift chambers

Wire drift chambers (Charpak, 1976) amplify the few electrons produced by ionization by an avalanche near the anode wires. Electron multiplication near the anode wire produces an easily processed signal which can be timed to produce a variety of precision spatial measurement systems. Electrodes are designed to provide electric fields in which the drift velocity can be well understood and provide small regions of high field that generate the electron avalanche from a primary ionization electron. Chambers range from small detectors to planar or cylindrical arrays of many square meters; 100-micrometer spatial resolution is routinely attained, as is multitrack resolution of better than 1 mm. Wire drift chambers can operate at the extremely high rates necessary in many fixed-target experiments and have been radiation hardened to operate in the harsh environment of high-luminosity proton colliders (CDF II Detector Technical Design Report, 1996). The coordinate measured by the drift time is normal to the wire. Low-precision measurements along the wire can be made utilizing resistive charge division and measuring the signal on both ends of the wires. Higher precision is achieved by small-angle stereo, necessitating the association of wire hits with tracks, which can be difficult in a busy environment. These systems can be used in a magnetic field for momentum measurement.

### 3. Proportional wire systems

Proportional wire systems operate in a mode where the signal is proportional to the primary ionization, thus measuring the energy-loss rate of the primary particle in the gas. *Avalanche systems* amplify the primary ionization to saturation, yielding large, very noise-immune signals. Such systems using single anode wires in moderate-resistivity tubes can give position signals by induction to strips with any geometry on the tube surface (Iarocci, 1983). They are widely used for muon detection with active areas of order 1000 square meters.

### 4. Time-projection chamber

In a time-projection chamber (Nygren, 1974) a sensitive volume is filled with a gas mixture with very low electron-attachment cross section. An applied uniform electric field drifts ionization electrons towards a two-dimensional array of detectors at one end. Tracks of charged particles are reconstructed from this detector array, with time of arrival at the array providing the

third coordinate. The time-projection chamber avoids most of the association difficulties of wire chambers and provides digitized pictorial images of events. The time-projection chamber has limitations in high-rate environments, as accumulated slow-moving positive ions distort the drift field.

#### 5. Semiconductor detectors

The development of high-resistivity silicon led to pn diodes that can directly detect the ionization caused by the passage of a charged particle. A minimum ionizing particle yields about 80 electron-hole pairs per micrometer of depleted silicon, or of order  $10^3$  electrons in a typical detector. The geometry of electrodes is nearly arbitrary, and detectors range from large-area diodes to "microstrips," arrays several cm long divided into diode units of width 25 to 100 micrometers. The overall scale is set by the size of the silicon wafer. Elaborate arrays of microstrips, with sophisticated low-mass space frame structures supporting the silicon stable to a few micrometers in space are used as vertex detectors. Since it is not yet possible to process complex transistor arrays on the detector wafers and maintain high resistivity, many connections must be made to nearby readout electronics. A vertex detector may have  $10^4$  to  $10^5$  channels, so power and thermal management of the electronics, as well as of the wire-bonded connections, are challenging. Two-dimensional information may be gained by connections to different sets of strips on either side of the silicon, or by using several one-sided arrays.

True pixel arrays are desirable because they give unambiguous space points, even in a dense particle jet. One approach uses charge-coupled devices (CCD's) fabricated from high-resistivity silicon. The simultaneous advantage and disadvantage of CCD's is that they are read out serially from a small number of readout nodes, thus requiring relatively little electronics but requiring tens of milliseconds for the readout process. For low-interaction-rate environments (such as  $e^+e^-$  linear colliders) this situation is ideal, and CCD's can provide 20-micrometer-sided pixels. Arrays of pixel diodes that are bump bonded to readout electronics are now being developed for Tevatron and Large Hadron Collider experiments. Such devices incorporate local smart readout to compress data, and can operate at high rates.

#### 6. Čerenkov radiation detectors

The simplest Čerenkov counters are velocity threshold devices using a medium whose index of refraction has been adjusted so that particles above some velocity generate radiation. The angle of radiation emission measures particle velocity. Focusing devices can send the radiation through a circular slit, allowing differential cuts on velocity. Such devices have relatively small acceptance and are used primarily in fixed-target experiments. A large step was taken with devices that actually image the cone of Čerenkov radiation on a sensitive focal plane to measure the Čerenkov angle. In composite large detectors on the scale of square meters, the focal

planes follow the momentum measurement and must detect single photons. In high-rate environments, the focal plane might be a pixellated array. The DELPHI experiment (Aarnio *et al.*, 1991) at LEP and the SLC Large Detector (SLD) at SLAC developed devices that contained low-electronegativity, high-photoabsorption organic molecules in large rectangular quartz-walled boxes. The Čerenkov photon converts to an electron in the organic vapor, and then drifts in an electric field of a few hundred V/cm to a wire chamber at the end of the box. The drift length is read out as time, and the conversion coordinates normal to the drift are read out by the wire number and by charge division on the wire.

#### 7. Transition radiation detectors

A charged particle traversing a boundary between materials differing in dielectric constant will emit photons. Thus detector components of sensitivity sharply increasing with  $\gamma$  can be constructed of sandwiched layers of gas and foils, with a photon detector, usually a heavy-gas wire drift chamber, facing the exit surface. In practice such detectors require  $\gamma > 10^4$  for adequate signals.

### VIII. DETECTOR SYSTEMS

Detector systems generally accomplish particle tracking, momentum measurement of charged particles, particle identification, and total-energy measurement of single particles or groups (jets) of particles. Additionally on-line and off-line data analysis is provided. Since optimal use of the accelerator has become important, detector systems have grown in geometric acceptance and measurement resolution to maximize information from each event and optimally use accelerator luminosity. Increases in the number of channels and data rates, and in measurement precision, have augmented costs and sizes.

Fixed-target experiments generally include beam definition, target, drift or decay region, and detectors. The size of such experiments ranges from emulsions to the long baseline of neutrino oscillations. While primary accelerated particles are protons and electrons (or their antiparticles), fixed-target experiments can utilize secondary beams of long-lifetime particles. The experimentalist controls, albeit within limits, beam momentum, momentum spread, spill time, intensity, backgrounds, and experimental geometry. For *collider experiments* almost all parameters save beam energy are fixed by the collider design; in some cases some control of beam polarization may be possible. As a generality, more luminosity, if consistent with background requirements, is always wanted.

The basic scale of collider detectors is set by the highest particle momentum to be analyzed. This is defined by the dimensions of the required magnetic analyzer and the range of the most penetrating particles (generally muons).

In general, at the energy frontier,  $e^+e^-$  detectors are smaller and simpler than the  $p-p$  (or  $p\bar{p}$ ) detectors;  $e^+e^-$  machines operate at significantly lower energies,

and total cross sections are much smaller, and there is usually less demand for forward acceptance with  $e^+e^-$  detectors. Radiation hardness and rate requirements are less challenging for  $e^+e^-$  detectors; such colliders produce far fewer than one interaction per crossing. In contrast, the Large Hadron collider proton collider is expected to have more than 10 events per crossing with a crossing rate of 25 MHz.

#### A. Momentum measurement: Magnet configurations for collider detectors

The detectors at the CERN Intersecting Storage Rings (Gicomelli and Jacob, 1981), the first of the large-scale  $pp$  colliders, used varied magnetic configurations, mostly of modest acceptance. The first large-scale cylindrically symmetric detector using a magnetic solenoid was the MKI at SPEAR at SLAC. All subsequent collider detectors except for the UA1 at the SPPS at CERN were cylindrically symmetric, mostly with solenoidal magnetic fields, although toroidal fields for muon momentum analysis have been used. This magnetic configuration leads to coaxial “barrels” of vertex detection, momentum measurement, particle identification, calorimetry, and muon measurement. Geometric variations include endcaps closing the barrels and additional downstream detectors to improve the forward acceptance, which is compromised in the solenoidal geometry.

Magnetic fields of 1.5 to 4 T produced by superconducting solenoids are now used or proposed, as are position resolutions of somewhat better than 100 micrometers, leading to tracker radii in the range of 1 to 3 meters.

#### B. Particle identification

Particle identification generally relies on measurements of velocity (or the relativistic factor  $\gamma$ ) or rests on observation of interactions (or their lack). Velocity (or  $\gamma$ ) measurements use time of flight (TOF) or the outputs from Cerenkov or transition radiation detectors and observation of ionization density ( $dE/dx$ ). For sufficiently slow particles, measurement of time of flight (TOF) is straightforward. A plastic scintillator with reasonably good geometry coupled to a photomultiplier can give time resolution below 100 ps (Benlloch *et al.*, 1990). The technique is limited by lengths of the flight path and by background.

#### C. Calorimetry (total-energy measurement)

Calorimeters are used to measure the energy and position of hadrons (charged or neutral), electrons, and jets, and to help identify leptons in hadronic jets. Electromagnetic calorimeters must be thick enough to develop, contain, and measure cascade showers induced by electrons and photons. Hadronic calorimeters must be substantially thicker to contain nuclear cascades. Angular resolution of the calorimeter can be critical, and since position resolution is limited by transverse cascade

shower dimensions, the calorimeter may become rather large. Calorimeter design requires optimization among performance parameters of energy, angle, and time resolution with radiation hardness, size, and cost. Calorimeters can be sampling or nonsampling, i.e., homogeneous. The sampling calorimeters alternate high-atomic-number metals for shower development with layers of a sensitive medium, e.g., scintillator, to sample the shower development. Homogeneous devices, practical only for electromagnetic calorimeters, utilize a uniform ionization-sensitive medium both to develop and to measure the energy of a shower, such as crystals of NaI. Crystals of lead tungstate have been developed for the Compact Muon Solenoid (CMS) electromagnetic calorimeter.

Statistical fluctuations in shower development and the corresponding fluctuations of the ionization in the sensitive medium limit the energy resolution of a sampling calorimeter. Thus the energy resolution will vary as  $E^{1/2}$  and as  $t^{1/2}$  where  $E$  is the incident-particle energy and  $t$  is the thickness of the radiator between samples. In homogeneous calorimeters, stochastic processes lead to a fractional energy resolution which varies as  $1/(E)^{1/4}$ , but leakage of the shower from the calorimeter, electronics noise, nonuniformity of light collection, and calibration errors add a constant term (which must be combined in quadrature). Sampling electromagnetic calorimeters achieve fractional energy resolutions in the range 10–15 %/ $E^{1/2}$ , while crystal calorimeters achieve 1–5 %/ $E^{1/4} \oplus 1–3$  %, where  $E$  is measured in GeV.

An electromagnetic shower can usually be contained in about 25 radiation lengths, corresponding to 15 cm of lead. Hadronic calorimeters require roughly 10 interaction lengths for containment of hadronic jets, corresponding to 112 cm of uranium or 171 cm of iron. Economics usually dictate a sampling calorimeter with liquid argon, scintillator, or wire chambers as the active medium. In addition to sampling statistics, the resolution of hadronic calorimeters is affected by their relative response to electromagnetic and hadronic showers, usually resulting in fractional energy resolutions of 50–75 %/ $E^{1/2}$ .

Many interesting variants on the basic designs have been developed. For example, liquid argon is extremely radiation hard, but the traditional electrodes of alternating layers of metal have relatively slow response because of their inductance. Folded electrodes in an accordion shape better approximate a transmission line and have been proposed for ATLAS and GEM (ATLAS Liquid Argon Calorimeter Technical Design Report, 1996). To improve resolution, scintillating fibers can be effectively cast into a lead matrix.

#### D. On-line analysis, data acquisition, and trigger systems

Increases in speed, density, and functionality in data-acquisition electronics, even *after* the widespread utilization of transistor circuits, are quite impressive. While most early and some modern experiments utilize standardized modular electronics, many larger experiments

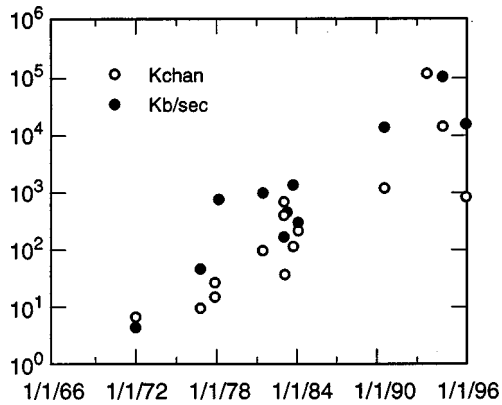


FIG. 4. Evolution of the number of detector signal channels with time, indicating growth of collider detector instrumentation capability over the last 24 years: open circles, number of electronic instrumentation channels in thousands; closed circles, design data rate in kilobytes per second to permanent storage. The date is that of the detector proposal or Technical Design Report.  $e^+e^-$ ,  $pp$ , and  $\bar{p}p$  detectors are included.

have improved performance and economics by using custom electronics integrated with the detectors proper. While channel densities are hard to compare, channel counts are shown versus proposal date for several detectors in Fig. 4. This growth with only moderate cost increase rests largely on continuing developments in circuit integration and computing technologies.

Most experiments produce raw data rates from the first stages of their electronics far too great to be recorded and subsequently analyzed. Trigger systems select a subset of events for recording, and the data-acquisition system compresses and corrects the data and associates data with different detector subsystems for each event. Most trigger systems have a three stage architecture: Level 1 is a fast, relatively simple hardware process that operates at the basic interaction rate of the machine and buffers a subset of events for Level 2, which uses more complex, slower algorithms to further reduce the rate for Level 3. Level 3 is usually a set of processors executing much of the nominal event-reconstruction code, thus making the full set of analysis cuts available. Level 1 implies fast, synchronous buffering of the event data, perhaps with only a subset of the data available to the Level-1 trigger processor. Level 2 requires slower, asynchronous buffering of the event data, and may have much of the data available to the processor. Level 3 has complete access to all of the data. The output of Level 3 is stored for off-line analysis, with data rates of roughly a megabyte per second.

The computation demands of many collider detectors continue to require leading-edge computation technology. Reconstruction of an  $e^+e^-$  event may require of order  $10^9$  instructions, and hadron collider events may need an additional order of magnitude. Most analyses require calculations of acceptances and efficiencies, implying generation and reconstruction of Monte Carlo data sets several times the size of the real data set. Finally, event samples may exceed  $10^9$  events, and data storage facilities of petabytes ( $10^{15}$ ) are proposed. For-

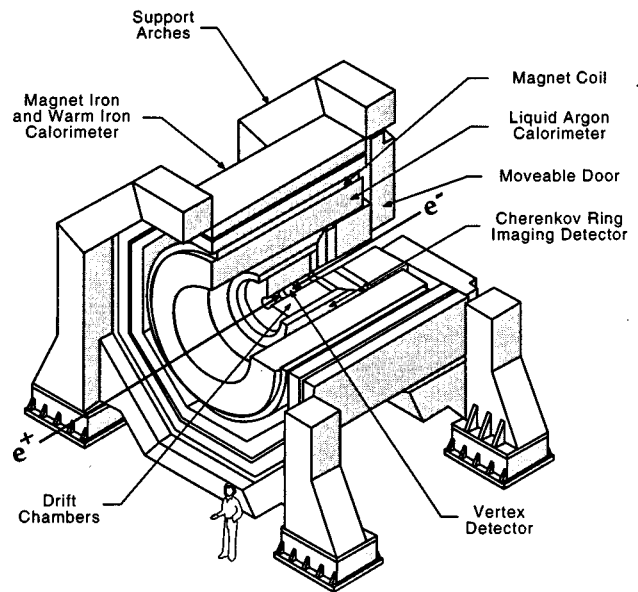
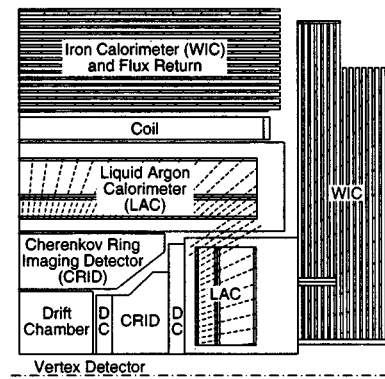


FIG. 5. Quadrant and cut-away views of the SLD detector.

tunately, event computation can easily run on arrays of computers on an event by event basis, and thus parallel "farms" are widely used.

#### E. The SLC Large Detector as an example of a collider detector system

The Stanford Linear Collider (SLC) collides bunches of about  $4 \times 10^{10}$   $e^-$  and  $e^+$  at 120 Hz, with a luminosity approaching  $2 \times 10^{30}$   $\text{cm}^{-2} \text{sec}^{-1}$ . A linear collider implies a very low true event rate and beam crossing rate; a very small luminous region in all three dimensions; and almost negligible radiation damage load on detector components. The SLC final focus system produces beam spots of about 1 micrometer horizontally and 0.5 micrometer vertically. Synchrotron radiation backgrounds are minimized by a masking system requiring multiple reflections for a photon to enter the detector. These features are exploited in the SLD design, shown in Fig. 5, to permit a CCD vertex detector with about  $3 \times 10^8$  pixels, a purely computational trigger, and a time-multiplexed data-acquisition system.

The vertex detector, consisting of 96  $18 \times 80$ -mm CCD's, is arrayed around a 25-mm-radius Be beam pipe. The position resolution of the vertex detector is dominated by multiple scattering at lower momenta. The solenoidal magnet has an inner diameter of 3 m and produces a magnetic field of 0.6 T. Charged-particle momenta are measured by an 80-layer cylindrical drift chamber extending radially from 20 cm to 1 m, and with a total length of 2 m, arranged in 10 superlayers of alternating stereo angle. The longitudinal coordinate is first estimated by charge division on the anode wires and then fitted using the stereo information. Momentum resolution of  $\Delta P/P = 0.01 \oplus 0.0026P_{\perp}$  (GeV/c) is achieved. SLD utilizes a Čerenkov ring imaging detector for particle identification. Three-standard-deviation separation between  $P$ 's and  $K$ 's is achieved from momenta of 1.5 to 5 and 9.5 to 45 GeV/c, and between  $K$ 's and  $\pi$ 's between 0.35 and 25 GeV/c. Next comes a sampling calorimeter of lead plates in liquid argon, arranged as towers that point projectively towards the vertex. An electromagnetic section is 22 radiation lengths deep, followed by an hadronic section approximately 3 interaction lengths deep. The total calorimeter is not thick enough to contain hadronic showers, but the tails are measured in an iron calorimeter that follows the aluminum solenoid. The iron calorimeter consists of 5-cm sheets of steel interleaved with limited streamer-mode chambers (Iarocci tubes). The chamber cathode surfaces are read out, on one side as a continuation of the liquid-argon calorimeter towers, and on the other as strips for a muon tracking system. The barrels are closed by endcaps of similar instrumentation.

The luminosity is monitored by small-angle Bhabha scattering measured by a pair of highly segmented tungsten-silicon diode calorimeters arranged as cylinders capturing the beam pipe about 1.5 m from the interaction point. Electron-beam polarization is measured by scattering a circularly polarized laser beam from the electron beam exiting the detector and measuring the asymmetry of the Compton-scattered electrons as the longitudinal polarization of the electrons is changed.

Essentially all electronics were customized for SLD. The basic architecture consists of preamplifiers feeding application-specific integrated circuits of switched-capacitor arrays to record each signal wave form. Subsets of this data are fed to a network of microprocessors to compute a trigger. In the trigger architecture described previously, Level 1 is the intrinsic SLC crossing rate, Level 2 is the microprocessor network, and Level 3 was not implemented since an acceptable rate for permanent storage is achieved by Level 2. After a trigger, data still held in the capacitor arrays are multiplexed to digitizers and transmitted via optical fibers to a network of about 600 microprocessors for data correction and compression.

## IX. THE FUTURE

Extension of existing accelerator and collider principles to higher performance requires advances in mag-

net technologies, superconducting technologies, etc. Detector systems must be able to operate in even more severe backgrounds. Today, work on new collider technologies is focused primarily on high gradients, and further issues concerning efficient conversion of power from the primary source to the beam must be addressed. Detector and data analysis methods are likely to match this evolution. During the next century of the American Physical Society these proposals should lead to practical designs for collider-based physics.

## ACKNOWLEDGMENTS

We should like to thank J. Jaros, A. Odian, A. Sessler, R. Siemann, and D. Whittum, for critical reading and helpful insights. Work was supported by Department of Energy contract DE-AC03-76SF00515.

## REFERENCES

- Aarnio, P., *et al.* (DELPHI Collaboration) 1991, Nucl. Instrum. Methods Phys. Res. A **303**, 233.  
 ATLAS Liquid Argon Calorimeter Technical Design Report, 1996, CERN/LHCC 96, 41.  
 Benlloch, J. M., M. V. Castillo, A. Ferrer, J. Fuster, E. Higon, A. Llopis, J. Salt, E. Sanchez, E. Sanchis, E. Silvestre, and J. Cuevas, 1990, Nucl. Instrum. Methods Phys. Res. A **290**, 327.  
 Bethe, H. A., 1932, Z. Phys. **76**, 293.  
 Bloch, F., 1933, Ann. Phys. **16**, 285.  
 Budker, G. I., 1969, Proceedings of the 7th International Accelerator Conference Program, Yerevan (1969).  
 CDF II Detector Technical Design Report, 1996, Fermilab Publ. 96/390-E.  
 Channell, P. J., 1982, Ed., *Laser Acceleration of Particles*, AIP Conf. Proc. No. 91 (AIP, New York).  
 Charpak, G., 1976, Nucl. Part. Phys. **6**, 157.  
 Chen, P., and R. J. Noble, 1986, in *Advanced Accelerator Concepts*, AIP Conf. Proc. No. 156, edited by F. E. Mills (AIP, New York), p. 222.  
 Christofilos, N., 1950, U.S. Patent #2,736,766.  
 Christofilos, N. C., R. E. Hester, W. A. S. Lamb, D. D. Reagan, W. A. Sherwood, and R. E. Wright, 1964, Rev. Sci. Instrum. **35**, 886.  
 Cockroft, J. D., and E. T. S. Walton, 1932, Proc. R. Soc. London, Ser. A **136**, 619.  
 Courant, E., M. S. Livingston, and H. Snyder, 1952, Phys. Rev. **88**, 1190.  
 DO Upgrade, 1996, Fermilab Pub. 96/357-E.  
 Giccomelli, G., and M. Jacob, 1981, in *CERN: 25 Years of Physics*, edited by M. Jacob (North-Holland, Amsterdam), p. 217.  
 Ginzton, E. L., W. W. Hansen, and W. R. Kennedy, 1948, Rev. Sci. Instrum. **19**, 89.  
 Iarocci, E., 1983, Nucl. Instrum. Methods Phys. Res. **217**, 30.  
 Kerst, D. W., 1940, Phys. Rev. **58**, 841.  
 Lawrence, E. O., and N. E. Edlefsen, 1930, Science **72**, 378.  
 Lawrence, E. O., and M. S. Livingston, 1932, Phys. Rev. **40**, 19.  
 Livingston, M. Stanley, 1954, *High-Energy Accelerators* (Interscience, New York), p. 151.  
 McMillan, E. M., 1945, Phys. Rev. **68**, 143.

- Nygren, D. R., 1974, in Proceedings of the PEP Summer Study, Lawrence Berkeley Laboratory, "The Time Projection Chamber: A new 4 Pi Detector for Charged particles," p. 58.
- Particle Data Group 1996, Phys. Rev. D **54**, 128,142.
- Raubenheimer, T. O., and F. Zimmermann, 1995, Phys. Rev. E **52**, 5487.
- Schoessow, P., 1994, Ed., *Advanced Accelerator Concepts*, AIP Conf. Proc. No. 335 (AIP, New York).
- Sloan, D. H., and E. O. Lawrence, 1931, Phys. Rev. **38**, 2021.
- Steinbeck, M., 1935, U.S. Patent #2,103,303.
- Tinlot, J., 1962, A storage ring for 10 BeV Mesons, SLAC-5, p. 165.
- Van de Graff, R. J., 1931, Phys. Rev. **38**, 1919.
- Waloschek, P., 1994, *The Infancy of Particle Accelerators: Life and Work of Rolf Wideroe* (Vieweg, Braunschweig).
- Wojcicki, S., 1998, NuMI-L-337 TDR, FNAL.
- Veksler, V. I., 1945, J. Phys (USSR) **9**, 153.